This is the accepted manuscript (postprint) of the following article:
Azizi, H., Eslami-Farsani, R., Vaezi, M. R., & Shokuhfar, A. (2024). Synthesis and effect of using silica fume particles on shear properties of basalt fibers-epoxy composites. *Polymer Composites*, *45*(2), 1619-1631.
https://doi.org/10.1002/pc.27877

Synthesis and effect of using silica fume particles on shear properties of basalt fibers-epoxy composites

Hosna Azizi[1], Reza Eslami-Farsani[1*], Mohammad Reza Vaezi[2], Ali Shokuhfar[1†]

[1] Faculty of Materials Science and Engineering, K. N. Toosi University of Technology, Tehran, Iran

[2] Department of Nanotechnology and Advanced Materials, Materials and Energy Research Center, Karaj, Iran

*Corresponding email: eslami@kntu.ac.ir

Abstract

In this study, the effect of the addition of silica particles modified with silane agent on the mechanical properties of basalt fibers-epoxy composites were studied with the interlayer shear strength (ILSS) test. In the first stage, silica fume particles were synthesized using the sol-gel method and surface modified using tri mercaptopropyl trimethoxy silane agent. The results of the characterization showed that the synthesized powder is nanometric scale, amorphous and high purity. The surface-modified silica fume particles (0, 2, 4, 6 wt.%) were distributed inside the epoxy matrix using a mechanical stirrer and ultrasonic waves. The hand lay-up method was used to fabricate composite samples, then the effect of adding these particles on the mechanical properties of basalt fibers-epoxy composites under interlayer shear loads was studied. The results of the research indicated that the addition of silica fume particles has a significant effect on improving the mechanical properties of basalt fibers-epoxy composites, and the greatest improvement in mechanical properties was achieved by adding 4 wt.% of modified silica fume particles. In the case of composites without SF particles, the shear strength was 34 MPa, which was increased to 40 MPa by adding 4 wt.% of SF particles (about 20% improvement). On the other hand, results demonstrated that the optimal distribution of silica fume particles within the polymer matrix performs an impressive role in improving the mechanical response of composite samples.

Highlights:

- The use of silica fume in the polymer composite is one of the research innovations.
- Silica fume is a super-fine spherical powder that is collected as a by-product.
- The silane is used to better distribute and optimal interaction of the silica fume in epoxy.
- Sol-gel is one of the methods to synthesis of silica fume.
- ILSS test was done to investigate the strength of the interface of basalt fibers and epoxy.

This is the accepted manuscript (postprint) of the following article:
Azizi, H., Eslami-Farsani, R., Vaezi, M. R., & Shokuhfar, A. (2024). Synthesis and effect of using silica fume particles on shear properties of basalt fibers-epoxy composites. *Polymer Composites*, *45*(2), 1619-1631.
https://doi.org/10.1002/pc.27877

Keywords: Basalt fibers, Mechanical properties, Polymer matrix composite, Silica fume, Sol-Gel

1- Introduction

Polymer composites are the most important group, ranging from high-end industries such as aircraft parts production to low-end industries such as dishwashers and etc. For this reason, they are the largest subset of composites [1-3]. Among natural fibers, basalt fibers due to their good strength properties, good adhesion between resin and fibers, sound insulation properties, high operating temperature range, lower price than carbon and Kevlar fibers, and also higher strength than optional glass fibers which are appropriate for utilization in various industries as reinforcement in the polymers [4-6].

Silica is used in various forms in various products, including silica powder, silicone gel, silica fume (SF), silica aerogel, etc. SF is a powder with a specific gravity of 200-300 kg/m^3 with a whitish-gray color that is a by-product of the ferrosilicon production process [7]. SF is a super-fine spherical powder that is collected as a by-product. These particles are about 1 μm and the average diameter is 0.1 μm. Today, SF is utilized in concrete, in multifarious industries such as detergent powders, coating powders, insulation powders, refractory ceramics, semiconductors, and textiles [8-10].

Regarding the use of SF in polymeric materials, good research has been accomplished, which will be mentioned in this section [11-16]. Pandian and Jeilani [11] interrogated the effect of waste SF addition at various contents on the dynamic mechanical behavior of jute fibers/epoxy composites and evinced that by adding 2 wt.% SF particles, the storage modulus and enhanced by 7% compared with unmodified composites.

Investigation of Alameri and Oltulu [12] demonstrated an improvement of 41% in compressive strength of SF/polyester composites by adding 5 wt.% of SF particles. By adding further SF particles a significant reduction in mechanical properties was observed due to the unfavorable distribution of these particles within the polymer matrix. In the research of Almadny et al. [13] the decrement in wear rate was obtained by adding SF and fly ash particles. In the case of SF particles In the case of fly ash addition, the at least wear rate was at 15%, and at higher contents, the wear rate increased.

Saleh et al. [14] studied the mechanical response of epoxy-containing SF and fly ash. SF and fly ash were admixed to the polymer matrix in 10-50 wt.%. In the case of SF-containing composites, the greatest improvement in tensile strength was obtained by adding 40 wt.% SF and higher amounts decayed the tensile strength. Mizan and Matsumoto [15] studied the effects of SF addition on the interfacial shear strength of concrete consisting of polymer cement mortar. The results of this study distinguished that the inclusion of 5 wt.% SF caused an improvement in the interfacial strength during which the shear strength increased from 0.94 to 2.01 MPa.

This is the accepted manuscript (postprint) of the following article:
Azizi, H., Eslami-Farsani, R., Vaezi, M. R., & Shokuhfar, A. (2024). Synthesis and effect of using silica fume particles on shear properties of basalt fibers-epoxy composites. *Polymer Composites*, *45*(2), 1619-1631.
https://doi.org/10.1002/pc.27877

Singh et al. [16] investigated the usage of SF as novel fillers in epoxy glass micro balloon syntactic foams. The results showed that the compressive strength of foams by adding 5 vol. % of SF increased from 65 to 80 MPa. On the other hand, flexural strength and toughness increased by 54 and 23%, respectively, by adding the same amount of SF.

Kaybal et al. [17] investigated the influences of the halloysite nanotubes (HNTs) addition and seawater aging on the bearing performance and failure behavior of basalt fibers reinforced epoxy nanocomposite materials. HNTs reinforcements remarkably improved the bearing strength of basalt fibers/epoxy composite laminates with an 18% increase. In addition, seawater aging drastically impairs the bearing response of composite laminates with an almost 45% reduction in bearing strength after 6 months of exposure. The HNTs reinforcement help to develop the bearing performance of basalt fibers/epoxy composites under static loading subjected to seawater environment.

Ulus et al. [18] investigated the impact of HNTs on shear and mode II fracture performances of the seawater aged basalt fibers reinforced epoxy composites. After six months of aging in seawater, the findings indicated that HNTs reinforced multi-scale composites exhibited 34 and 46% higher shear strength and mode II delamination toughness compared to the neat specimens. Moreover, according to the dynamic-mechanical analysis, higher glass transition temperatures (8%) were obtained for the multi-scale composites. One of the more significant findings to emerge from this study is that the toughening mechanisms of HNTs such as pull-out, crack deflection, and crack pinning were attributed to the enhancement in the mechanical performances.

Examination of the research revealed that the most common application of SF particles is in the concrete industry and cement-based composites. Research on applying SF in polymeric materials has shown that most research has focused on the addition of SF in pure polymers such as polystyrene, vinyl esters, etc. Hence, the main scope of this research is first the synthesis of SF by sol-gel method and structural studies of SF and then the effect of adding surface-modified SF with silane agent on the mechanical behavior of basalt fibers-epoxy composites under interlaminar shear loading.

2- Experimental procedures

2-1- Materials

In this research, epoxy resin (ML-506) and polyamine hardener were used as polymer bases. The reason for choosing this resin is due to its low viscosity improved the distribution of silica particles inside it. For the fabrication of composite samples, basalt fibers fabric with satin texture (Basaltex Co.) with a surface density of 300 g/m^2 were utilized as fiber reinforcement in the composites.

This is the accepted manuscript (postprint) of the following article:
Azizi, H., Eslami-Farsani, R., Vaezi, M. R., & Shokuhfar, A. (2024). Synthesis and effect of using silica fume particles on shear properties of basalt fibers-epoxy composites. *Polymer Composites*, *45*(2), 1619-1631.
https://doi.org/10.1002/pc.27877

The silane coupling agent is used in order to better distribute the SF particles in the epoxy and also for the optimal interaction between them. Tri mercaptopropyl trimethoxy silane with chemical formula $C_6H_{16}O_3SSi$ (Sigma Aldrich Co.) was used to modify the surface of SF particles in the composite polymer matrix.

Liquid sodium silicate was used as a silica agent with a density of 1.35 g/cm^3 and a boiling point of more than 100°C (Merck Co.) for the synthesis of SF particles. Also, nitric acid with a molecular weight of 63 g/mol and a purity of 65%, methanol with a purity of 99% and hexane ($C_6H_{14} \Rightarrow C_6H_{14}$) with a purity of 95% and a molecular weight of 86 g/mol (all from Qatran Chemical Co.) were used.

2-2- Synthesis of silica fume

On a laboratory scale, first, 30 g of sodium silicate solution was diluted with deionized water in a laboratory beaker until the solution reached a concentration of 4 g/lit of silica (pH=12.8), then nitric acid was added to the prepared solution using a dropper until it turns into a gel (pH=11). The prepared hydrogel was aged overnight in deionized water. Then, to remove sodium ions almost completely, the gel was washed six times with deionized water and with the help of a paper filter. In the next step, the gel was placed in methanol to replace its structural water, and this process was done five times and each time for 12 hours. In the next step, hexane was replaced with methanol, and then the previous process was repeated, with the difference that at the end of this step, 10 g of trimethylchlorosilane was added to the silica gel, and at the end, it was dried at 85°C for 6 hours. It was heated again for 12 hours at a temperature of 95°C to remove the hydrophobic agent [19-21].

2-3- Surface modification of silica fume

At first, 5 g of silane agent was added to 100 ml of a solution containing 95 ml of methanol, and the silane agent was mixed with the solution for 15 minutes by a mechanical stirrer. In the next step, 5 g of silica particles were added to the solution and the particles were mixed with the resulting solution for 30 minutes again by a mechanical stirrer. Finally, the resulting mixture was placed in a vacuum oven at 100°C for 24 hours. It should be noted that SF modified by this method was used to make composite samples [22, 23].

2-4- Fabrication of composite specimens

In order to distribute the SF in the matrix, the epoxy resin was first diluted by adding high purity alcohol as a diluting agent, which helps to better disperse the SF particles during the process and lower the viscosity of the resin. SF particles with specific weight amounts (0, 2, 4, and 6 wt.%) were added to the epoxy resin, and the particles were mixed for 30 minutes using a mechanical stirrer (Fintech Co.) with a power of 1500 rpm [24]. After finishing the stirring process, the mixture of resin and SF particles was applied in order to break the extant agglomerates of ultrasonic waves using an ultrasonic probe device (Fapan Co.) under a power of 120 W and a frequency of 24 kHz. For fabricating the composites, the hand lay-up method was utilized during which 12 layers of basalt fibers fabric with a volume ratio of 50% were used. Finally the samples were placed at ambient temperature for 3-4 hours to cure the epoxy.

2-5- Microstructural and Characterization studies

In order to investigate the microstructure of SF synthesized by the sol-gel method as well as the fracture surface of composite samples, an emission scanning electron microscope (FE-SEM, Mira TESCAN) with a working voltage of 15 kV was used.

To investigate the structure of SF synthesized, an X-ray diffraction (XRD, Unisantis XMD 300) device with CU Kα radiation under 30 kV voltage and 30 mA current, was used. For investigating the surface modification process of SF particles and the formation of functional groups on the surface of the particles, FT-IR analysis (Bruker infrared spectrometer) was employed in the wavelength range of 500-4000 cm^{-1} and with a sensitivity of 4 cm^{-1}.

In this research, Brunauer-Emmett-Teller (BET) analysis (Autosorb-1-mp, Quantachrome Co., USA) was used to investigate the amount of porosity and gas absorbed in SF powder. In this test, after placing the cell containing the target sample in the liquid nitrogen tank, the amount of gas absorbed by the material was calculated by gradually increasing the nitrogen gas pressure in each step [25].

2-6- Inter-laminar shear test

In order to investigate the strength of the interface between the basalt fibers and the epoxy base reinforced with surface-modified SF particles, the interlayer shear strength (ILSS, Koopa, 100 kN, Iran) was calculated based on the ASTM D2344 standard [26]. According to the standard, a sample with a rectangular cross-section and dimension of 50 mm × 10 mm × 5 mm was placed on two lower supports that have a fixed distance from each other, and then a central load was introduced into the sample from above at a rate of 2 mm/min.

This is the accepted manuscript (postprint) of the following article:
Azizi, H., Eslami-Farsani, R., Vaezi, M. R., & Shokuhfar, A. (2024). Synthesis and effect of using silica fume particles on shear properties of basalt fibers-epoxy composites. *Polymer Composites*, *45*(2), 1619-1631.
https://doi.org/10.1002/pc.27877

To measure the ILSS of the samples, equation 1 is used, in which P, b, and d are the maximum load in N, and the width and thickness of the samples in mm. It should be noted that equations 2 and 3 were used to calculate the width and length of the samples.

$$\text{ILSS}=\frac{3P}{4bd} \quad (1)$$

$$b=2d \quad (2)$$

$$L=6d \quad (3)$$

3- Results and discussion

3-1- Characterization of silica fume

3-1-1- Microstructural analysis of synthesized silica fume

The microstructure of the synthesized SF is shown in Fig. 1 at different magnifications. The particle size distribution of SF has been shown to have a particle size of 11-25 nm.

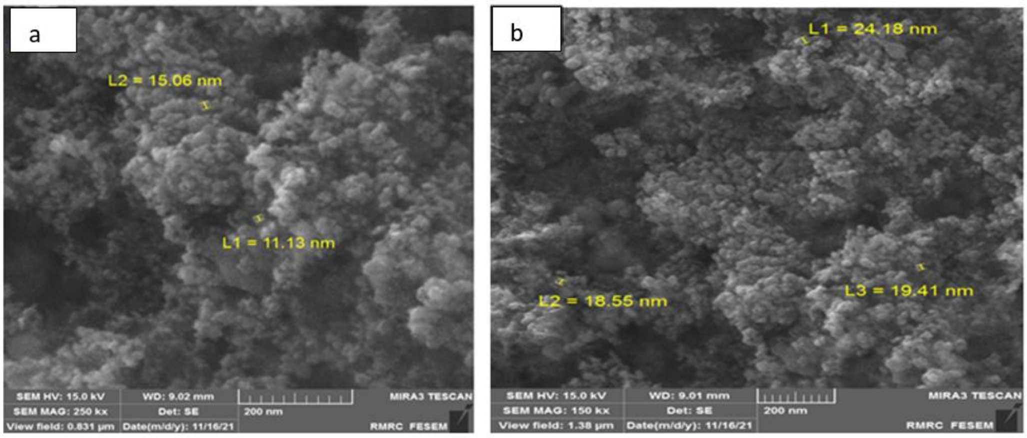

Figure 1. The size distribution of synthesized silica particles in, a) 250,000, b) 150,000 times magnifications.

3-1-2- XRD analysis

Fig. 2 shows the results of XRD analysis on SF powder synthesized by the sol-gel method. Based on the XRD results, it is observed that the obtained silica structure is generally amorphous, which is related to the rapid condensation of volatile silica and surface tension silicon in the phase transition [27]. The broad peak obtained at an angle of about 22 degrees indicates amorphous silica with nanometer size, and this result was compared with similar articles, which all showed the same result [28, 29].

This is the accepted manuscript (postprint) of the following article:
Azizi, H., Eslami-Farsani, R., Vaezi, M. R., & Shokuhfar, A. (2024). Synthesis and effect of using silica fume particles on shear properties of basalt fibers-epoxy composites. *Polymer Composites*, *45*(2), 1619-1631.
https://doi.org/10.1002/pc.27877

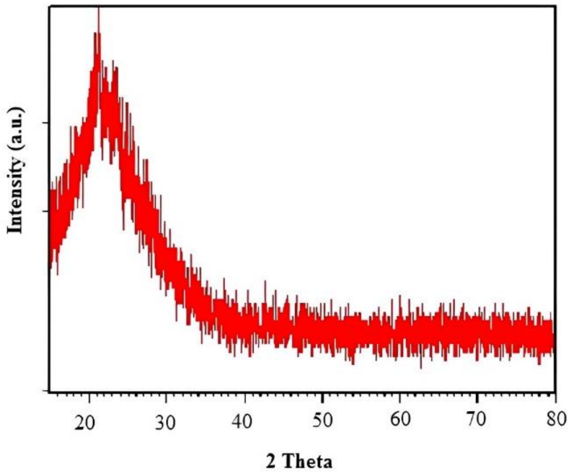

Figure 2. The results of XRD analysis on SF powder synthesized by sol-gel method.

3-1-3- EDS analysis

In Fig. 3, the results of energy dispersive spectroscopy (EDS) analysis on synthesized SF powder and Table 1, elemental analysis of SF synthesized by sol-gel method, are shown, which is consistent with the results of XRD analysis. The EDS curve of amorphous SF contains elements of silicon and oxygen, which indicates that the synthesized SF was obtained with high purity, during which the weight percentage of silicon was 57.43. The presence of silicon and oxygen peaks confirms the synthesis of SF particles from sodium silicate. Also, acid treatment using nitric acid led to the removal of alkaline impurities from the synthesized powder [30]. This was because silica is insoluble in acid, while other impurities such as sodium, iron, and potassium were dissolved in hydrochloric acid due to acid treatment.

This is the accepted manuscript (postprint) of the following article:
Azizi, H., Eslami-Farsani, R., Vaezi, M. R., & Shokuhfar, A. (2024). Synthesis and effect of using silica fume particles on shear properties of basalt fibers-epoxy composites. *Polymer Composites*, *45*(2), 1619-1631. https://doi.org/10.1002/pc.27877

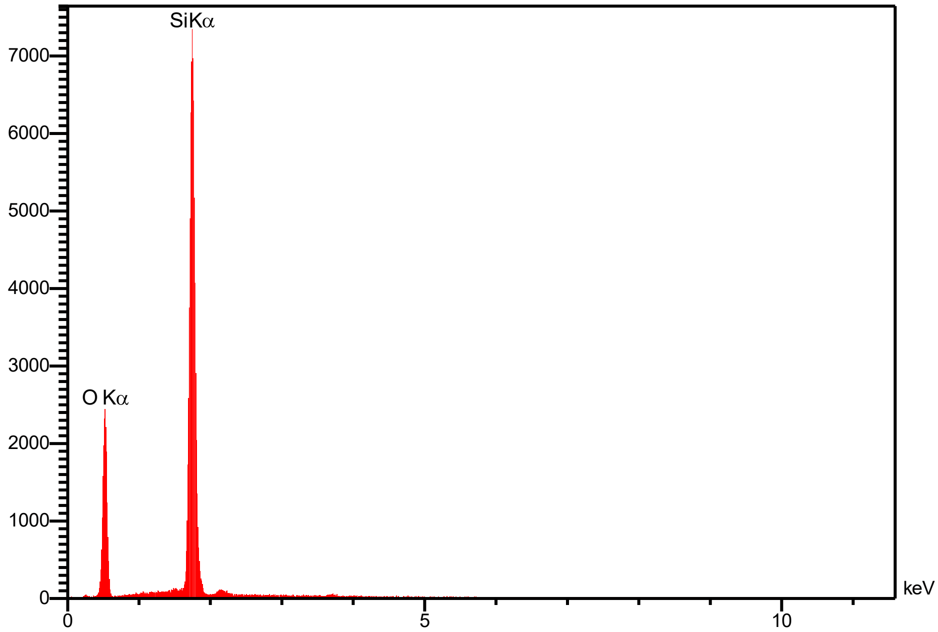

Figure 3. The results of EDS analysis on synthesized SF powder.

Table 1. Elemental analysis of SF synthesized by sol-gel method

Element	X-ray kind	Atomic percent	Weight percent
Si	Kα	70.48	57.43
O	Kα	29.52	42.57

Fig. 4 shows the result of image analysis and linear analysis of the synthesized SF powder in map-EDS. The EDS map analysis is shown the weight percentage of silicon and oxygen is displayed according to the distance in a specific range of 0-2 µm. It shows that the trend of changes in the weight percentage of silicon is decreased to 1 µm, while the trend of changes in the weight percentage of oxygen is upward manner to 1µm. Finally in the range of 1-1.5 µm, is shown a decrease in oxygen weight percentage.

This is the accepted manuscript (postprint) of the following article:
Azizi, H., Eslami-Farsani, R., Vaezi, M. R., & Shokuhfar, A. (2024). Synthesis and effect of using silica fume particles on shear properties of basalt fibers-epoxy composites. *Polymer Composites*, *45*(2), 1619-1631.
https://doi.org/10.1002/pc.27877

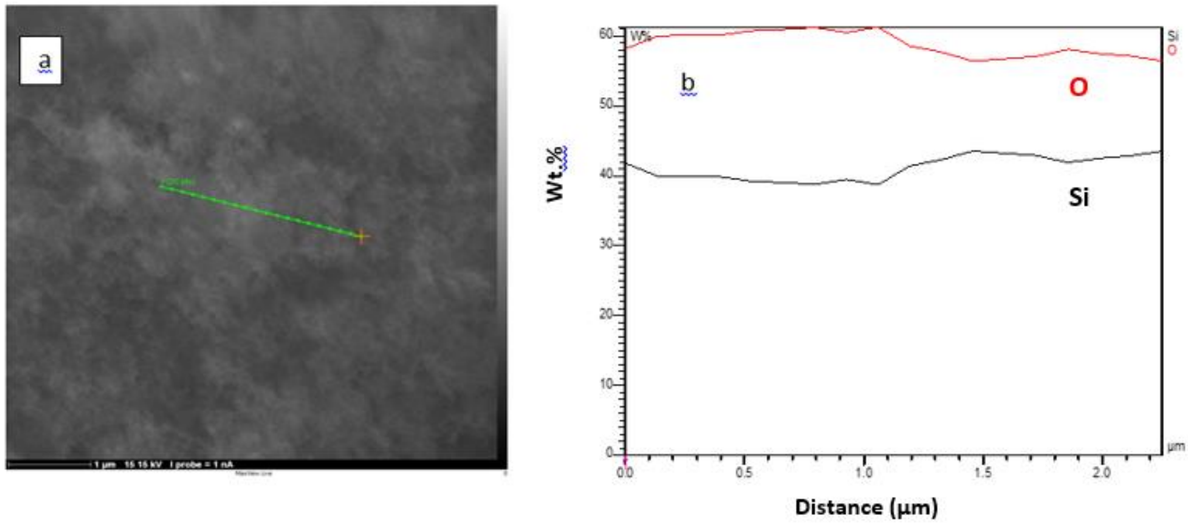

Figure 4. Changes in weight percentage of silicon and oxygen elements of the synthesized SF powder in map-EDS analysis, a) image analysis, and b) linear analysis, of the sample.

3-1-4- BET analysis

Fig. 5 shows the porosimetry curves of nitrogen absorption and desorption of SF powder obtained by the sol-gel method. Adsorption is usually expressed through isotherms, which is equivalent to the amount of adsorbed material on the absorbent surface and is a function of the pressure or concentration of the adsorbed material under constant temperature conditions. As it can be seen, the obtained curve is the fifth type of absorption isotherm, according to which, considering that a hysteresis loop is formed in the image, it can be claimed that the prepared SF particles have meso and cylindrical cavities [31]. The absorption and desorption branches related to the silica particles are almost horizontal and almost parallel to each other, which can be caused by the uniformity in the size of the mesopores. At the point of twist, the first absorbent layer is completed and the absorption of subsequent layers begins. The sharpness of each absorption step depends on the homogeneity of the absorbent surface and temperature. There is a relationship between the shape of the hysteresis loop and the distribution and size of the holes. The hysteresis loop obtained in this research is of the third type, which does not show the limitation in absorption at high relative pressures, that the structure has planar holes along with micro holes. The rejection branch in this type of hysteresis has a steep slope that leads to the closing of the loop, which is called the tensile strength effect [32-34].

This is the accepted manuscript (postprint) of the following article:
Azizi, H., Eslami-Farsani, R., Vaezi, M. R., & Shokuhfar, A. (2024). Synthesis and effect of using silica fume particles on shear properties of basalt fibers-epoxy composites. *Polymer Composites*, *45*(2), 1619-1631.
https://doi.org/10.1002/pc.27877

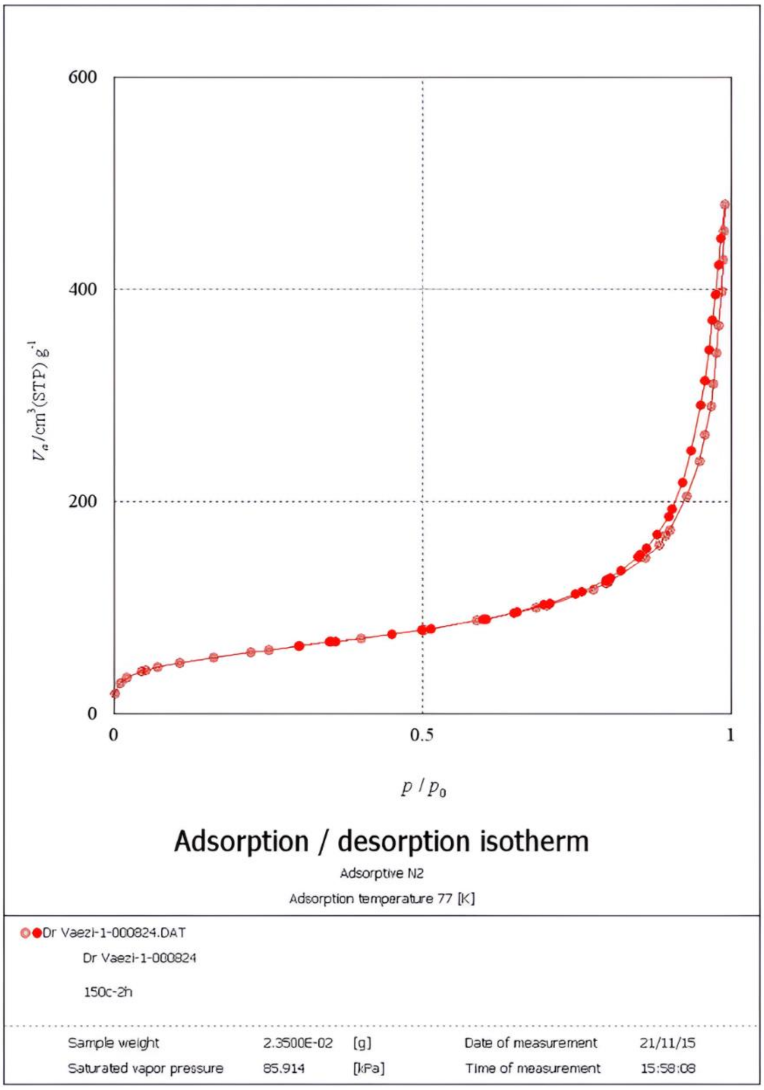

Figure 5. Isothermal absorption and desorption graph of SF.

Fig. 6 shows the BET curve of amorphous SF synthesized by the sol-gel method. As can be seen, the curve at the relative pressure of 0-0.5 is a straight line with a positive slope, which indicates that the BET chart can be used with good accuracy. At relative pressures greater than 0.25, capillary condensation begins and at very low relative pressures, only a single layer is formed.

Surface characteristics of the SF obtained by the BET method are shown. The surface area of the synthesized SF powder was 202 m^2/g, the absorbed volume of nitrogen gas was 46.503 cm^3/g and the BET constant was 110.42.

This is the accepted manuscript (postprint) of the following article:
Azizi, H., Eslami-Farsani, R., Vaezi, M. R., & Shokuhfar, A. (2024). Synthesis and effect of using silica fume particles on shear properties of basalt fibers-epoxy composites. *Polymer Composites*, *45*(2), 1619-1631.
https://doi.org/10.1002/pc.27877

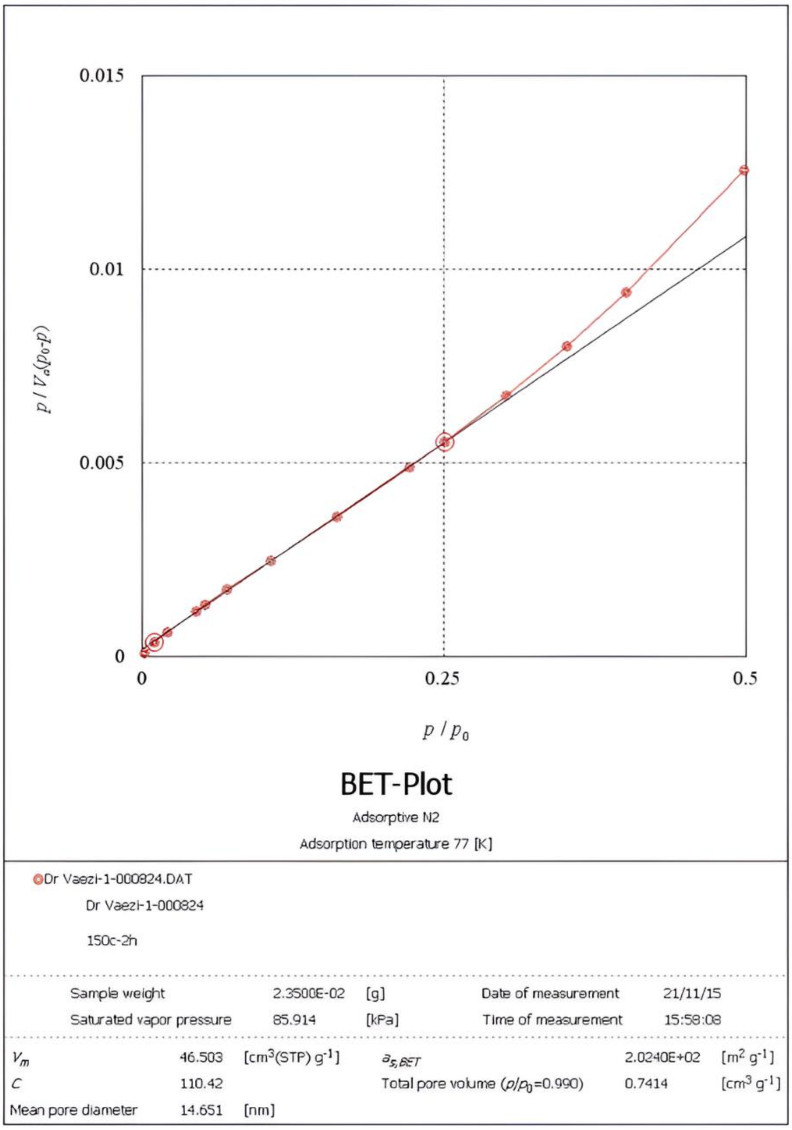

Figure 6. BET curve of synthesized SF.

To more closely examine the cavities in the SF particles and to ensure the formation of mesopores in the synthesized powder, the size distribution of the pores has been investigated based on the Barrett, Joyner, Halenda (BJH) model according to Fig. 7. These graphs indicate the concentration of the hole size in the dimensions of 1.21 nm, that is, in the meso range. Also, in this model, the volume of the holes was 0.7175 cm^3/g. On the other hand, the narrowness of the hysteresis loop showed that the porous mesoporous system is formed by the narrow size distribution of the holes, which was confirmed by the results of BJH analysis [35].

This is the accepted manuscript (postprint) of the following article:
Azizi, H., Eslami-Farsani, R., Vaezi, M. R., & Shokuhfar, A. (2024). Synthesis and effect of using silica fume particles on shear properties of basalt fibers-epoxy composites. *Polymer Composites*, *45*(2), 1619-1631.
https://doi.org/10.1002/pc.27877

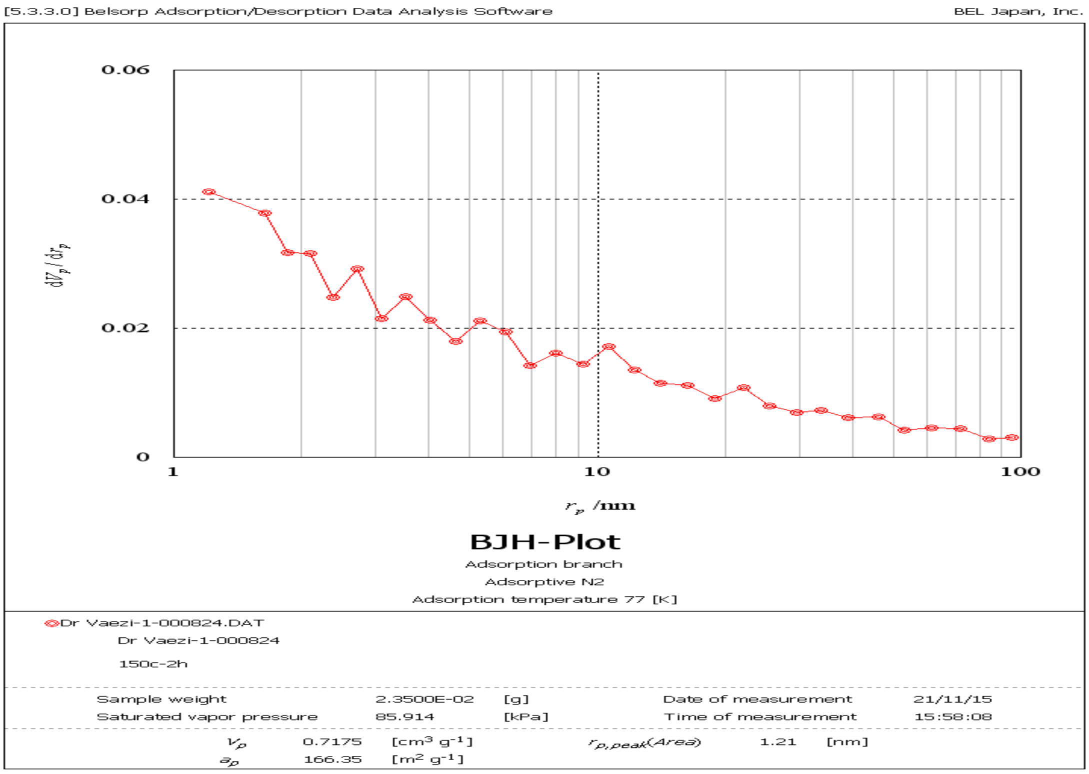

Figure 7. BJH curve of synthesized SF.

3-1-6- FT-IR analysis

Fig. 8 shows the infrared spectroscopy of unmodified and silane-modified SF particles. About the unmodified particles (Fig. 8-a), the peaks obtained at 1634.56 cm^{-1} and 3434.7 cm^{-1} were related to the bending and stretching vibrations of the H-O-H bond, respectively. The peaks created at wave number 809.34 cm^{-1} and 1517.49 cm^{-1} were caused by the stretching and bending vibration of Si-OH, respectively, which is related to the characteristics of silica. The absorption peaks created at 1109 cm^{-1} and 473.82 cm^{-1} were respectively related to the asymmetric stretching and bending vibration of siloxane (Si-O-Si) [36, 37]. The presence of Si-OH and Si-O-Si vibration bands indicated the amorphous state of the synthesized silica particles.

In modified SF particles (Fig. 8-b), in addition to the presence of the previous peaks, new absorption peaks appeared in wave numbers 917.5 cm^{-1} and 2933.02 cm^{-1}. The obtained peaks in the wave numbers 917.5 cm^{-1} and 2933.02 cm^{-1} were respectively related to CH_2 stretching vibration. This article clearly showed that the surface of the SF particles was successfully modified by the silane agent [38].

This is the accepted manuscript (postprint) of the following article:
Azizi, H., Eslami-Farsani, R., Vaezi, M. R., & Shokuhfar, A. (2024). Synthesis and effect of using silica fume particles on shear properties of basalt fibers-epoxy composites. *Polymer Composites*, *45*(2), 1619-1631.
https://doi.org/10.1002/pc.27877

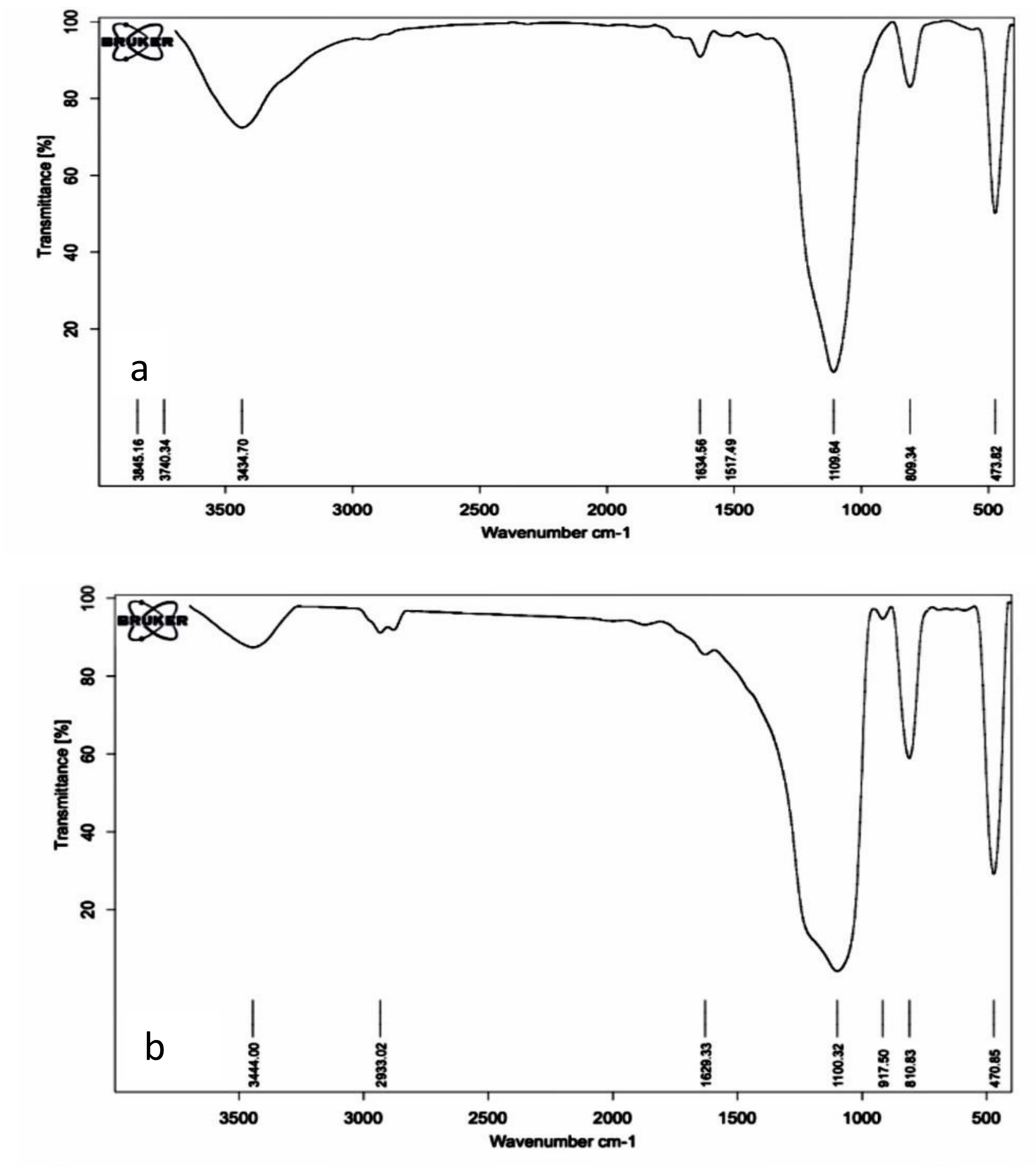

Figure 8. FT-IR spectroscopy results of SF, a) raw powder, b) modified with silane.

3-2- Interlaminar shear test results

Fig. 9 shows the effect of SF particles modified with silane on the interlaminar shear strength (ILSS) of composites reinforced with basalt fibers. As can be seen, by adding SF inside the epoxy matrix, the ILSS increased at first and then decreased. In this regard, for composites

This is the accepted manuscript (postprint) of the following article:
Azizi, H., Eslami-Farsani, R., Vaezi, M. R., & Shokuhfar, A. (2024). Synthesis and effect of using silica fume particles on shear properties of basalt fibers-epoxy composites. *Polymer Composites*, *45*(2), 1619-1631. https://doi.org/10.1002/pc.27877

without SF particles, the shear strength was 34 MPa, which was increased to 40 MPa by adding 4 wt.% of SF particles, and in this case, the shear strength was improved by 20%.

Ulus et al. [39] investigated the effect of the addition of HNTs on the shear strength of basalt fibers-epoxy composites. The shear strength of the basalt fibers/neat epoxy composite is calculated as 36.1 MPa. The addition of 2 wt.% HNTs in the epoxy matrix are found to increase the shear strength up to 42.9 MPa, which is approximately 19% higher than that of the sample without HNTs. The comparison of the results indicates that the amount of improvement in mechanical properties caused by the addition of SF to the matrix and the addition of HNTs to the matrix is approximately the same.

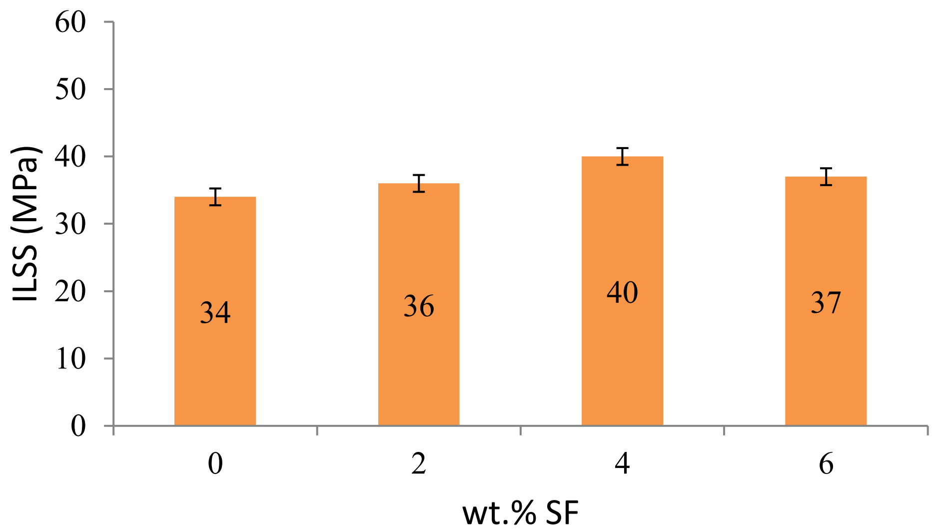

Figure 9. Effect of adding SF particles on ILSS of composites.

The reason for the observed increase in ILSS due to the addition of SF particles can be related to the improvement of the strength of the base as well as the interface between the basalt fibers and the matrix. The change in the residual stresses in the matrix owing to the presence of silica reinforcement particles caused pressure on the surface of the fibers, which subsequently caused strong adhesion between the fibers and the matrix. On the other hand, the presence of silica particles acted as a coupling factor between the matrix and the fibers. In this way helped to improve the adhesion between the fibers and the matrix, which is shown schematically in Fig. 10. Also, the presence of these particles in the matrix prevented the growth and creation of cracks and improved the shear properties of the final composite [40]. At higher weight percentages (6 wt.%), due to the formation of SF agglomerates, a decrease

This is the accepted manuscript (postprint) of the following article:
Azizi, H., Eslami-Farsani, R., Vaezi, M. R., & Shokuhfar, A. (2024). Synthesis and effect of using silica fume particles on shear properties of basalt fibers-epoxy composites. *Polymer Composites*, *45*(2), 1619-1631.
https://doi.org/10.1002/pc.27877

in interlayer shear strength was expected. The agglomerates at the interface between the fibers and the matrix help to separate them during loading, and as a result, the mechanical properties of the composite decrease. In fiber-reinforced composite materials, load transfer takes place through the interface between the matrix and the reinforcement. The proper distribution of silica particles in the epoxy matrix leads to an increase in the adhesion between the matrix and the fibers. Increasing the adhesion of fibers and the matrix increases the strength of the interface, which makes the load transfer well, as a result, the mechanical properties of the composite increase [41].

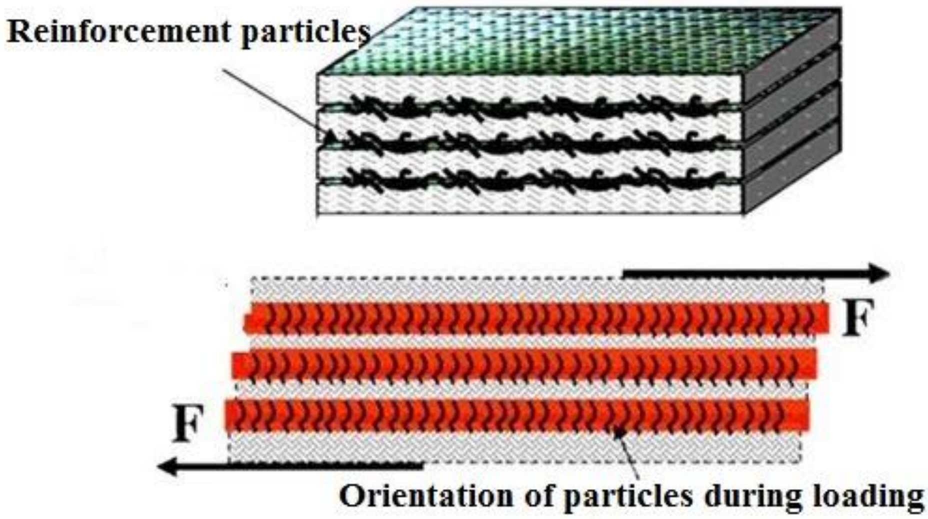

Figure 10. Influence of reinforcing particles in improving the interlaminar shear strength of the composite sample [34].

In fiber-reinforced composites, the surface of the fibers and the interface between the matrix and the fibers are stress concentration areas, and these stress concentration areas are mainly areas for crack initiation [42]. On the other hand, the strength of the interface determines the length of the stress transfer. A stronger interface results in a shorter stress transfer length and therefore a greater portion of the fibers bear the applied load, which leads to an increase in the load-bearing capacity. On the contrary, the weaker interface has a longer stress transfer length and a small part of the fibers can bear the applied load, which leads to a decrease in the load-bearing capacity [43].

3-3- Fracture surface studies

This is the accepted manuscript (postprint) of the following article:
Azizi, H., Eslami-Farsani, R., Vaezi, M. R., & Shokuhfar, A. (2024). Synthesis and effect of using silica fume particles on shear properties of basalt fibers-epoxy composites. *Polymer Composites*, *45*(2), 1619-1631.
https://doi.org/10.1002/pc.27877

SEM images of control sample (that doesn't contain SF) and a sample containing SF particles distributed in the matrix are shown in Fig. 11. For the control samples (Fig. 11-a), the smoothness of the fracture surface of the fibers indicates a weak interface between the epoxy matrix and the reinforcing fibers. Meanwhile, for the samples containing SF particles (Figs. 11-b-d), after the composite failure, some of the polymer matrix phase is attached to the surface of the basalt fibers. This event indicates the favorable adhesion between the epoxy matrix and the fibers. It is due to the proper distribution of silica fume particles inside the epoxy resin. The conclusion of the comparison of these two images is that the mechanism of control samples is the interface separation. While in the samples with the matrix reinforced with SF particles, the dominant failure mechanism is the cracking of the matrix [44, 45].

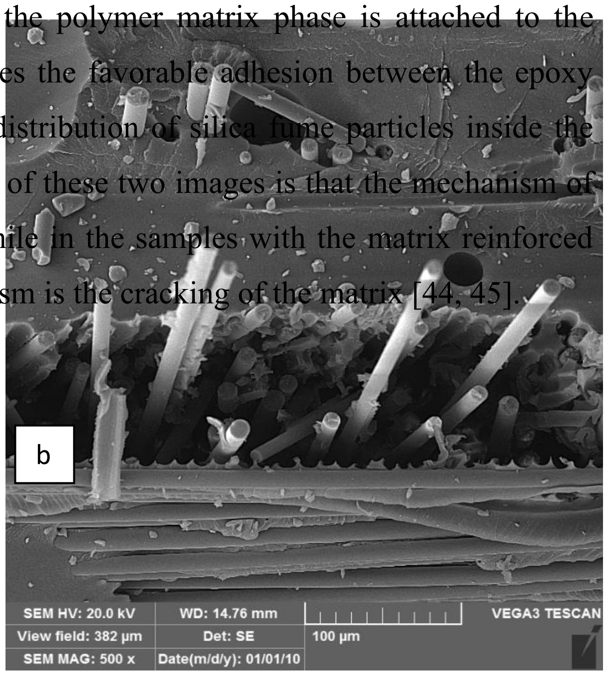

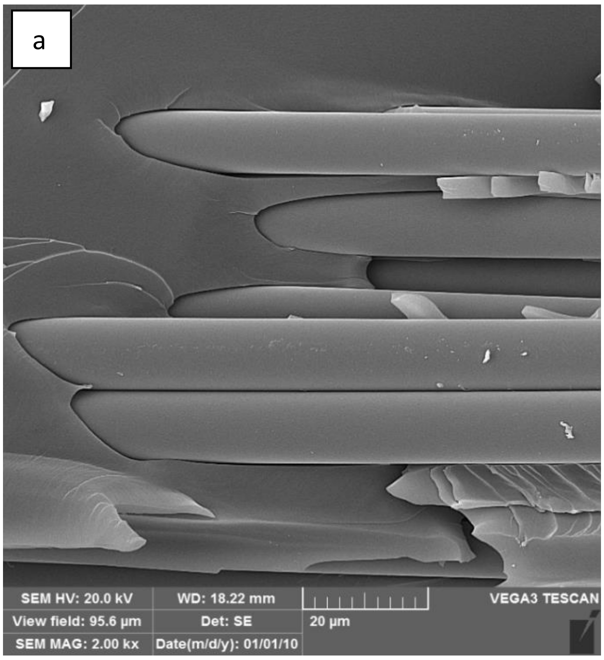

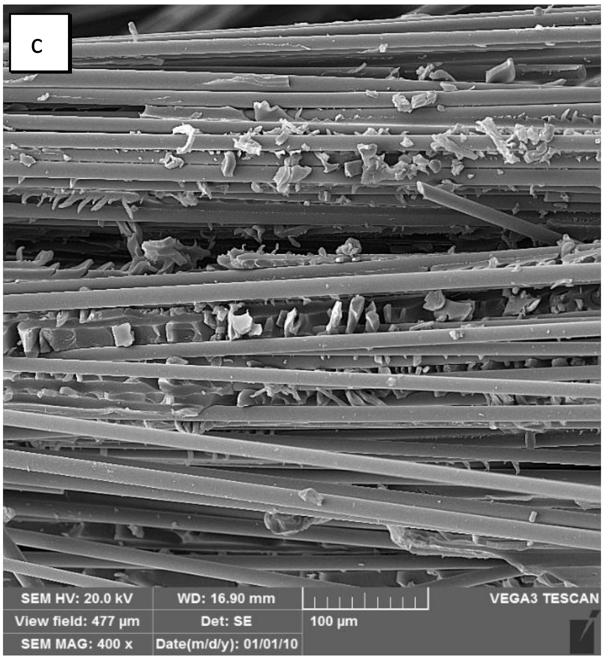

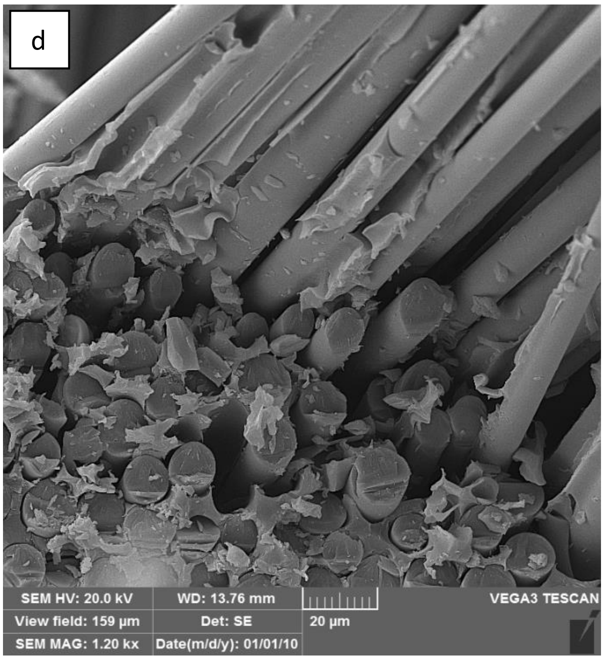

This is the accepted manuscript (postprint) of the following article:
Azizi, H., Eslami-Farsani, R., Vaezi, M. R., & Shokuhfar, A. (2024). Synthesis and effect of using silica fume particles on shear properties of basalt fibers-epoxy composites. *Polymer Composites*, *45*(2), 1619-1631.
https://doi.org/10.1002/pc.27877

Figure 11. SEM image of fracture surface, a) control composite in 2 kx, b) composite reinforced with 4 wt.% of SF in 500 x, c) 400 x, d) 1.20 kx.

Fig. 12 shows the microscopic images of the epoxy matrix (neat epoxy), and (containing 4 wt.% SF). In connection with samples reinforced with SF, there are many shear bands in the matrix, which was due to the high resistance of SF reinforcing particles to crack growth, while for the pure epoxy matrix; the fracture surface is smooth, which is a sign of brittle failure. In relation to the matrix containing SF, there are irregularities in the fracture surface and the crack deviation caused by loading can be seen. This is one of the main reasons for the increment in energy absorption of the samples including SF particles [46-48].

Nanoparticles can deflect the crack and exhibit a rougher surface pattern. Crack pinning and crack path deflection, were determined as liable mechanisms for the modified adhesive joint's higher rigidity and less energy absorption. The crack pinning mechanism is based on the interaction of a crack and, rigid nanoparticles that behave as an impassable obstacle, hinder the crack propagation and provide an additional toughness. As a result of these interactions, the crack is pinned or deflected, thus causing improved toughness [49, 50].

Fig. 13 shows the fracture surface of the epoxy-containing 6 wt.% of silica particles in higher magnification, which confirms the presence of agglomerates of these particles in the composite matrix, was the main cause of the loss of mechanical properties of basalt fibers-epoxy composites.

This is the accepted manuscript (postprint) of the following article:
Azizi, H., Eslami-Farsani, R., Vaezi, M. R., & Shokuhfar, A. (2024). Synthesis and effect of using silica fume particles on shear properties of basalt fibers-epoxy composites. *Polymer Composites*, *45*(2), 1619-1631.
https://doi.org/10.1002/pc.27877

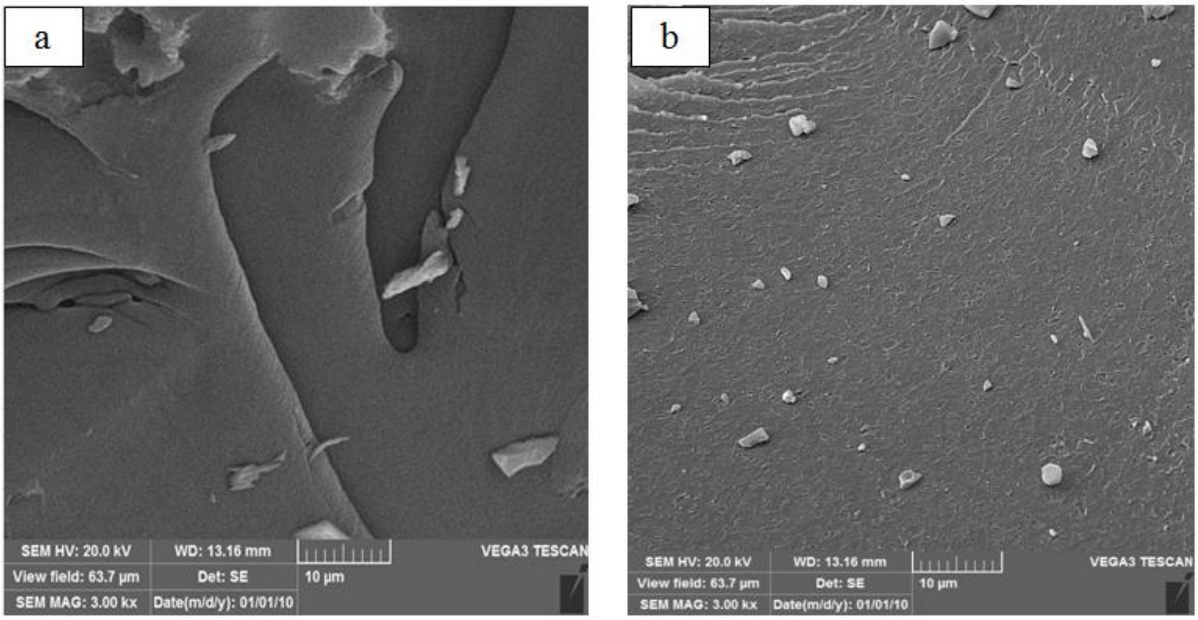

Figure 12. SEM image of the matrix, a) neat epoxy, b) epoxy containing 4 wt.% SF.

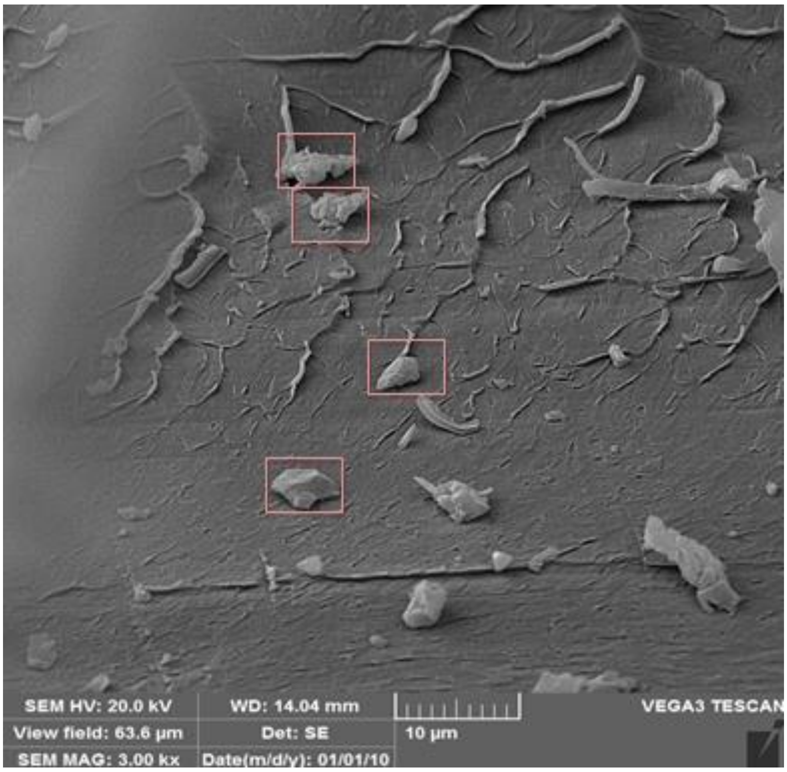

Figure 13. Agglomeration of SF in the epoxy matrix.

4- Conclusion

This is the accepted manuscript (postprint) of the following article:
Azizi, H., Eslami-Farsani, R., Vaezi, M. R., & Shokuhfar, A. (2024). Synthesis and effect of using silica fume particles on shear properties of basalt fibers-epoxy composites. *Polymer Composites*, *45*(2), 1619-1631.
https://doi.org/10.1002/pc.27877

In this research, at first, silica fume particles were synthesized using sol-gel. Then the effect of the addition of silica particles modified with silane agent on the mechanical properties of basalt fibers-epoxy composites under interlayer shear loading was studied. For this purpose, the modified silica fume particles in 0, 2, 4, and 6 wt.% were distributed inside the composite matrix.

Microstructural investigations of the synthesized powder showed that the structure of the synthesized powder is amorphous and has high purity. The size of the particles is on the nanometer scale (11-25 nm). The results of infrared spectroscopy analysis revealed that the silica particles were successfully modified with a silane agent. The addition of silica fume particles (4 wt.%) has a significant effect on improving the interlaminar shear strength. This strength increased by 20% compared to the composite without silica particles. The downfall in the mechanical properties of basalt fibers-epoxy composites for the distribution of 6 wt.% of silica fume was due to the clumping of these particles within the composite.

References

[1] K. P. Kumar and A. S. J. Sekaran, Some natural fibers used in polymer composites and their extraction processes: A review, Journal of Reinforced Plastics and Composites, vol. 33 ,pp. 1879-1892, 2014.

[2] R. Alderliesten, On the development of hybrid material concepts for aircraft structures, Recent Patents on Engineering, vol. 3, pp. 25-38, 2009.

[3] S. Nunna, P. R. Chandra, S. Shrivastava, and A. Jalan, A review on the mechanical behavior of natural fiber-based hybrid composites of Reinforced Plastics and Composites, vol. 31, pp. 759-769, 2012.

[4] R. H. Wu, The application of basalt fiber in building materials, Advanced Materials Research, vol. 450, pp. 499-502, 2012.

[5] Z. Guo, N. Hao, L. Wang and J. Chen, Review of basalt-fiber-reinforced cement-based composites in China: their dynamic mechanical properties and durability, Mechanics of Composite Materials, vol. 55, pp. 107-120, 2019.

[6] V. V. Prasad and S. Talupula, A review on reinforcement of basalt and aramid (Kevlar 129) fibers, Materials Today: Proceedings, vol. 5, pp. 5993-5998, 2018.

[7] S. Fallah, and M. Nematzadeh, Mechanical properties and durability of high-strength concrete containing macro-polymeric and polypropylene fibers with nano-silica and silica fume, Construction and building materials, vol. 132, pp. 170-187, 2017.

[8] S. Karamikamkar, H. E. Naguib, and C. B. Park, Advances in precursor system for silica-based aerogel production toward improved mechanical properties, customized morphology and

multifunctionality: A review, Advances in colloid and interface science, vol. 276, p. 102101, 2020.

[9] A. V. Zanfir, G. Voicu, A.-I. Bădănoiu, D. Gogan, O. Oprea and E. Vasile, Synthesis and characterization of titania-silica fume composites and their influence on the strength of self-cleaning mortar, Composites Part B: Engineering, vol. 140, pp. 157-163, 2018.

[10] G. L. Golewski, Energy savings associated with the use of fly ash and nano additives in the cement composition, Energies, vol. 13, issue. 9, p. 2184, 2020.

[11] C. K. A. Pandian and H. S. Jailani, Dynamic and vibrational characterization of natural fabrics incorporated hybrid composites using industrial waste silica fumes, International Journal of Polymer Analysis and Characterization, vol. 24, pp. 721-730, 2019.

[12] I. Alameri and M. Oltulu, Mechanical properties of polymer composites reinforced by silica-based materials of various sizes, Applied Nanoscience, vol. 10, pp. 4087-4102, 2020.

[13] H. A. Almadny, A. Alkhafaji, and L. A. Alasadi, Effect of silica-based wastes on wear rate and hardness properties of epoxy composites as a construction material, Key Engineering Materials, vol. 895, pp. 31-40, 2021.

[14] N. A. Saleh, M. Al-Maamori and M. B. Al-Jebory, Evaluating the mechanical properties of Epoxy resin with Fly ash and Silica fume as fillers, Advances in Physics Theories and Applications, vol. 30, pp. 1-7, 2014.

[15] M. H. Mizan and K. Matsumoto, Studying the influence of silica fume on bond strength of the pcm-concrete interface under shear stress condition, Materials, vol. 15, issue. 4, pp. 1473, 2022

[16] V. V. Singh, P. Jaiswal and A.V. Ullas, Mechanical properties of silica fume reinforced epoxy glass micro balloons syntactic foams, Materials Today: Proceedings, vol. 46, pp. 672-676, 2021.

[17] HB. Kaybal, H. Ulus, and A. Avcı, Seawater aged basalt/Epoxy composites: improved bearing performance with halloysite nanotube reinforcement. Fibers and Polymers, vol. 22, pp.1643-1652, 2021.

[18] H. Ulus, HB. Kaybal, V. Eskizeybek, A. Avcı, Significantly improved shear, dynamic-mechanical, and mode II fracture performance of seawater aged basalt/epoxy composites: The impact of halloysite nanotube reinforcement, Engineering Science and Technology, an International Journal, Vol. 24, No. 4, pp.1005-1014, 2021.

[19] Y. Pan, S. He, X. Cheng, Z. Li, C. Li, Y. Huang, L. Gong, A fast synthesis of silica aerogel powders-based on water glass via ambient drying. Journal of Sol-Gel Science and Technology, vol. 82, pp. 594-601, 2017.

[20] B. Koozegar Kaleji, S. Mirzaee, S. Ghahramani, S. Rezaie, N. Hosseinabadi, A. Fujishima, Sol–gel synthesis of Sn/Fe co-doped TiO 2 nanoparticles: study of structural, optical and photocatalytic properties, Journal of Materials Science: Materials in Electronics, vol. 29, pp. 12351-12359, 2018.

[21] L. Nevřivová, D. Zemánek, Study of the Mineralogical Composition of an Alumina–Silica Binder System Formed by the Sol–Gel Method, Materials, vol. 16, No. 15, pp. 5466, 2023.

[22] R. Suntako, Effect of modified silica fume using MPTMS for the enhanced EPDM foam insulation, Polymers, vol. 13, issue. 17, pp. 2996, 2021.

[23] U. U. Pillai and K.B. Anand, Performance evaluation of polyurethane-nano silica modified cement mortar, Materials Today: Proceeding, vol. 46, pp. 4788-4794, 2021.

[24] H. Khosravi, and R. Eslami-Farsani, Enhanced mechanical properties of unidirectional basalt fiber/epoxy composites using silane-modified Na+- montmorillonite nano clay, Polymer Testing, Vol. 55, pp. 135-142, 2016.

[25] Determination of the specific surface area of solids by gas adsorption- BET method, ISO 9277, 2010.

[26] Short-beam strength of polymer matrix composite materials and their laminates, ASTM D 2344, 2000.

[27] O. Vogut, N. Ukrainczyk, and E. Koenders, Effect of silica fume on metakaolin geo polymers sulfuric acid resistance, Materials, vol. 14, issue. 18, pp. 5396, 2021.

[28] R. Malathy, R. Shanmugam, M. Chung, S. H. Kim and M. Prabakaran, Mechanical and microstructural properties of composite mortars with lime silica fume and rice husk ash Processes, vol. 10, issue. 7, pp. 1424, 2022.

[29] R. Maddalena, C. Hall, and A. Hamilton, Effect of particle size n the formation of calcium silicate hydrate using thermal analysis, Thermochimica Acta, vol. 672, pp.142-149, 2019.

[30] Y. Wang, T. Chen and C. Yan, Reinforced performances of polymethyl methacrylate/silica fume composite spherical particles used as ultra-lightweight proppants, Journal of Reinforced Plastics, vol. 34, pp. 672-683, 2015.

[31] Y. Zhang, H. Qi and J. Sun, Preparation and characterization of a porous silicate material from silica fume, Korean Journal of Chemical Engineering, vol. 34, pp. 3185-3194, 2017.

[32] L. Wang, M. Jin, F. Guo, Y. Wang, and S. Tang, Pore structural and fractal analysis of the influence of fly ash and silica fume on the mechanical property and abrasion resistance of concrete, Fractals, vol. 29, pp. 214003, 2021.

[33] S. Nasreen, U. Rafique, S. Ehrman, and M. A. Ashraf, Synthesis and characterization of mesoporous silica nanoparticles for environmental remediation of metals, PAHs and phenols, Ekoloji, vol. 27, pp. 1625-1637, 2018.

[34] K. Yang, Mohanapriya. V, Jana. K, Yuji. S, Sana. U, Ick-Soo. K, and J. Yao, Structural analysis of embedding polyethylene glycol in silica aerogel, Microporous and Mesoporous Materials, vol. 310, pp. 110636, 2021.

[35] V. Shekle S. S. Bhagade and S. A. Mandavgane, Mesoporous silica from rice husk ash:, Bulletin of Chemical Reaction Engineering, vol. 5, pp. 63-67, 2010.

[36] R. A. Bakar, R. Yahya and S. N. Gan, Production of high purity amorphous silica from rice husk, Procedia Chemistry, vol. 19, pp. 189-195, 2016.

[37] T. H. Mokhothu, A.S. Luyt and M.Messort, Preparation and characterization of EPDM/silica nanocomposites prepared through non-hydrolytic sol-gel method in the absence and presence of a coupling agent, Express Polymer Letters, vol. 8, pp. 809–822, 2014.

[38] S. Y. Lee, J. S. Kim, S. H. Lim, S. H. Jang, D. H. Kim, N. H. Park, J. W. Jung and J. Choi, The investigation of the silica-reinforced rubber polymers with the methoxy type silane, Polymers, vol. 12, pp. 3058-3066, 2020.

[39] H. Ulus, HB. Kaybal, V. Eskizeybek, A. Avcı, Halloysite nanotube reinforcement endows ameliorated fracture resistance of seawater aged basalt/epoxy composites, Journal of composite materials, Vol. 54, No. 20, pp. 2761-2779, 2020.

[40] S. Huang, Q. Fu, L. Yan and B. Kasal, Characterization of interfacial properties between fiber and polymer matrix in composite materials, Journal of Materials Research and Technology, vol. 13, pp. 1441-1484, 2021.

[41] J. K. Kim and Y. W. Mai, Engineered interfaces in fiber reinforced composites, Elsevier, 1998.

This is the accepted manuscript (postprint) of the following article:
Azizi, H., Eslami-Farsani, R., Vaezi, M. R., & Shokuhfar, A. (2024). Synthesis and effect of using silica fume particles on shear properties of basalt fibers-epoxy composites. *Polymer Composites*, *45*(2), 1619-1631.
https://doi.org/10.1002/pc.27877

[42] S.Houshyar, A. Shanks and A. Hodzic, Modelling of polypropylene fiber-matrix composites using finite element analysis, Express Polymer Letters, vol. 3, pp. 2-12, 2009.

[43] M. F. Uddin and C. T. Sun, Strength of unidirectional glass/epoxy composites with silica nanoparticle-enhanced matrix, Composites Science and Technology, vol. 68, pp. 1637–1643, 2008.

[44] M. Alsaadi and A. Jabbar, Nanosilica inclusion effects on the mechanical and dynamic behavior of fiber reinforced carbon/Kevlar with epoxy resin hybrid composites, Composites Part B: Engineering, vol. 152, pp. 169-179, 2018.

[45] H. Azizi, R. Eslami-Farsani, Study of mechanical properties of basalt fibers/epoxy composites containing silane-modified nanozirconia, Journal of Industrial Textiles, Vol. 51, No. 4, pp. 649–663, 2021.

[46] E. Kazemi-Khasragh, F. Bahari-Sambran, S.M.H. Siadati, R. Eslami-Farsani, and S. Arbab Chirani, The Effects of surface-modified graphene nanoplatelets on the sliding wear properties of basalt fibers-reinforced epoxy composites, Journal of Applied Polymer Science, Vol. 136, No. 39, pp. 47986, 2019.

[47] E. Kazemi-Khasragh, F. Bahari-Sambran, S.M.H. Siadati, R. Eslami-Farsani, High-velocity impact response of basalt fibers/epoxy composites containing graphene nanoplatelets, Fibers and Polymers, Vol. 19, No. 11, pp. 2388-2393, 2018.

[48] A. Abdi, R. Eslami-Farsani, and, H. Khosravi, Evaluating the mechanical behavior of basalt fibers/epoxy composites containing surface-modified $CaCO_3$ nanoparticles, Fibers and Polymers, Vol. 19, No. 3, pp. 635-640, 2018.

[49] H. Ulus, HB. Kaybal, F. Cacık, V. Eskizeybek, A. Avcı, Fracture and dynamic mechanical analysis of seawater aged aluminum-BFRP hybrid adhesive joints, Engineering Fracture Mechanics, Vol. 268, pp. 108507, 2022.

[50] H. Ulus, HB. Kaybal, F. Cacık, V. Eskizeybek, A. Avcı, Effect of long-term stress aging on aluminum-BFRP hybrid adhesive joint's mechanical performance: Static and dynamic loading scenarios, Polymer Composites, Vol. 43, No. 8, pp. 5301-5318, 2022.